FEASIBILITY OF POLYANILINE ELECTRODES FOR LITHIUM TITANATE BASED ENERGY STORAGE DEVICES

by

Rahul Krishna Prasad

B.A.Sc., The University of British Columbia, 2008

A THESIS SUBMITTED IN PARTIAL FULFILLMENT OF
THE REQUIREMENTS FOR THE DEGREE OF

MASTER OF APPLIED SCIENCE

in

THE FACULTY OF GRADUATE STUDIES

(Electrical and Computer Engineering)

THE UNIVERSITY OF BRITISH COLUMBIA

(Vancouver)

June 2011

Abstract

A long lasting energy storage device with energy density rivalling batteries would be very useful in many applications, especially ones where device replacement is difficult or expensive. Devices based on lithium titanate electrodes are considered promising in this regard, as lithium titanate electrodes have very long cycle lives. In this thesis, the feasibility of using the conducting polymer polyaniline in conjunction with a lithium titanate electrode to build a battery-supercapacitor combination energy storage device is considered, since polyaniline is also expected to have a high cycle life, due to its supercapacitor-like charge storage mechanism. Various methods for fabricating a polyaniline electrode are considered, and the deposition of polyaniline onto a stainless steel substrate from an aqueous solution was used. The polyaniline electrode, upon being tested in a non-aqueous solution containing lithium ions, was found to have a specific capacitance and a specific capacity of roughly 220 F/g and 85 F/g respectively. Nuclear magnetic resonance tests were used to find that the lithium ions do not dope the polyaniline and drive its oxidation state changes; therefore, the electrolyte in the proposed device must accommodate all the lithium ions emitted from the lithium titanate electrode. A simulation is presented, based on experimental data from each electrode tested separately, which estimates the energy density of the complete device to be 22.8 Wh/kg and the cost to be $560/kWh. This energy density is more than two-thirds that of a lead-acid battery and the cost is competitive with lithium-ion batteries, so the device is considered viable in applications where long-lasting devices are of utmost importance.

Preface

All work reported in this thesis was performed by the author apart from the results for the lithium titanate electrode in Chapter 3. These are based on work conducted in Dr. John Madden's laboratory at UBC by the author in collaboration with Niloofar Fekri and Chi Wah Eddie Fok. The experimental work was shared amongst us equally. The design of the experimental setup in this chapter was done by Chi Wah Eddie Fok. The nuclear magnetic resonance tests in Chapter 2 are based on work conducted in Dr. Carl Michal's laboratory. Dr. Michal's assistance with these experiments is gratefully acknowledged. Many thanks to Boris Niraula for his help and encouragement with the polyaniline electrode work.

Table of Contents

List of Tables

List of Figures

Acknowledgements

I thank my supervisor, Dr. John Madden, and my parents, for their patient support even during times of frustration or difficulty.

I would also like to thank Boris Niraula, for his helpful input on the handling of polyaniline, Dan Sik Yoo, for his help with the initial setup of the three-electrode experimental cell, Dr. Carl Michal, for his assistance with the nuclear magnetic resonance tests and Eddie Fok and Niloofar Fekri, for their assistance in fabricating and testing the lithium titanate electrode.

I am also grateful to the Natural Sciences and Engineering Research Council of Canada (NSERC) for their funding through a Postgraduate Scholarship (PGS M).

1 Introduction

This chapter will introduce the aim and background of this project, explain the basic difference between batteries and capacitors and describe the nature of the energy storage device proposed in this thesis, along with its expected performance characteristics.

1.1 Aim and Background

The importance of energy storage devices is likely to increase in the new few decades as they find greater use in applications such as grid storage, hybrid electric vehicles, distributed generation systems, remote applications and backup systems. The energy storage demands in these applications are usually met by using batteries, which typically offer high energy density. However, supercapacitors offer certain unique advantages which may make them desirable in certain applications.

When batteries are charged, electrical energy has to be converted to chemical potential energy through chemical reactions. Chemical reactions are also required when converting this stored potential energy back to the electrical form. The repeated cycles of chemical reactions wear down the battery over time. Due to this, batteries suffer from limited cycle lives and often require frequent and expensive replacements. These replacements are even more expensive in situations where the battery is in a remote location, such as on a buoy at sea.

Supercapacitors may offer advantages in this regard because of the fundamentally different way in which capacitors store charge. By avoiding the chemical reactions that occur in energy conversions in batteries, supercapacitors offer the possibility of building longer lasting energy storage devices. In this thesis, the use of a conducting polymer material called polyaniline is considered for use as an electrode in an energy storage device. Although charge storage in polyaniline is not strictly capacitive, it is found to behave very much like a capacitive electrode. Due to this, it offers high cycle life which can be harnessed to build a long-lasting energy storage device.

The viability of combining a polyaniline electrode with a lithium titanate electrode to build a complete energy storage device is considered in this thesis. This device is a battery-supercapacitor combination and aims to combine the high energy density properties of batteries with the high lifetimes typical of supercapacitors. As is explained in the following sub-sections of this chapter, this energy storage device is expected to have long cycle life and battery-like energy density.

1.2 Conventional Capacitor Mechanism

In a typical parallel-plate capacitor, two conducting plates are held apart by a dielectric (insulating) material, as depicted in Fig. 1.1.

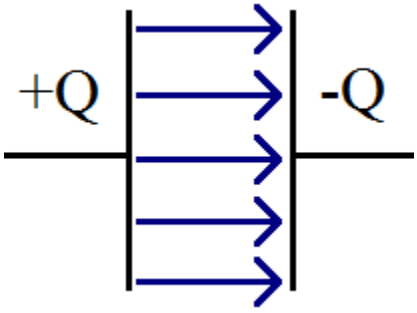

Fig. 1.1 A conventional capacitor.

When a voltage is applied between the two plates, charges of opposite polarity accumulate at each end. An electric field is thus produced across the dielectric which enables the storage of energy. This is accomplished without any chemical reactions as in batteries. The capacitance is given by:

$$C = \frac{Q}{V}.$$

The energy stored in the capacitor is given by:

$$Energy = \frac{1}{2}CV^2.$$

1.3 Basic Supercapacitor Mechanism

In a supercapacitor, two porous electrodes are held apart by an insulating porous material called a separator. Because the electrodes are made of porous materials, the electrolyte is able to penetrate inside these electrodes and enter the pores. This is shown in Fig. 1.2 below.

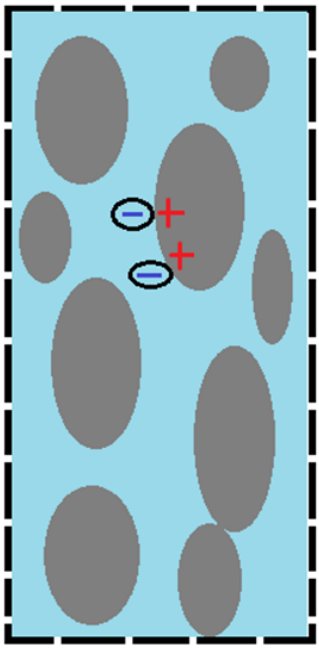

Fig. 1.2 Cross-sectional diagram of a porous electrode. The grey ovals represent the porous material, while the blue space represents the electrolyte filling the pores. When a potential is applied to the porous material, an electrochemical double layer is formed across the interface between the porous material and the electrolyte.

When a potential is applied to the electrode, ions of the opposite polarity, present in the electrolyte in the pores, are attracted towards the electrode. An electrochemical double layer is formed in the pores of the electrode by this charge build-up along the interface between the electrode and the solution in the pores. This double layer can be modelled by a parallel-plate capacitor. This model offers two reasons why a supercapacitor has such high capacitance: (1) In a parallel-plate capacitor, the capacitance is inversely proportional to the distance between the plates. Therefore, since the double layer is extremely thin (on the order of 10 nanometres), the capacitance per area is very high.

(2) Since a porous electrode offers a large surface area for the interface between the electrode and the electrolyte, the double layer can be thought of as very large capacitors (each corresponding to a pore) in parallel with one another. Since the capacitances of capacitors in parallel simply add up, the electrode tends to offer very high capacitance.

As with a regular capacitor, energy is stored in a supercapacitor in electric fields created through the build-up of charge (across the double-layer). This is different from a battery, where electrical energy is converted to chemical potential energy through chemical reactions for energy storage. This chemical potential energy must be converted back to electrical energy through chemical reactions when the energy needs to be used. These chemical reactions tend to degrade the battery and reduce its cycle life. A supercapacitor is able to achieve a much longer cycle life due to its fundamentally different method of storing energy.

1.4 Energy Storage Device Proposed

In this thesis, an energy storage device is proposed where the working electrode is a polyaniline electrode and the counter electrode is a lithium titanate electrode. Since the two electrodes are not identical, this device is called a hybrid device. It is a combination of a battery and a supercapacitor in this case.

Charge storage in polyaniline does not follow a strictly capacitive mechanism, since chemical reactions do occur where charges enter or leave the structure of the polyaniline as it changes state (due to change in potential). This is shown in Fig. 1.3 below. However, the charge transfer reactions very much resemble the charge transfer mechanism in a capacitor. Polyaniline is a pseudocapacitive material and the extent of faradaically admitted charge into the polyaniline is almost directly proportional to the applied voltage [1]. The capacitive behaviour of the polyaniline is demonstrated in section 2.4.3 where cyclic voltammetry tests are done on the polyaniline.

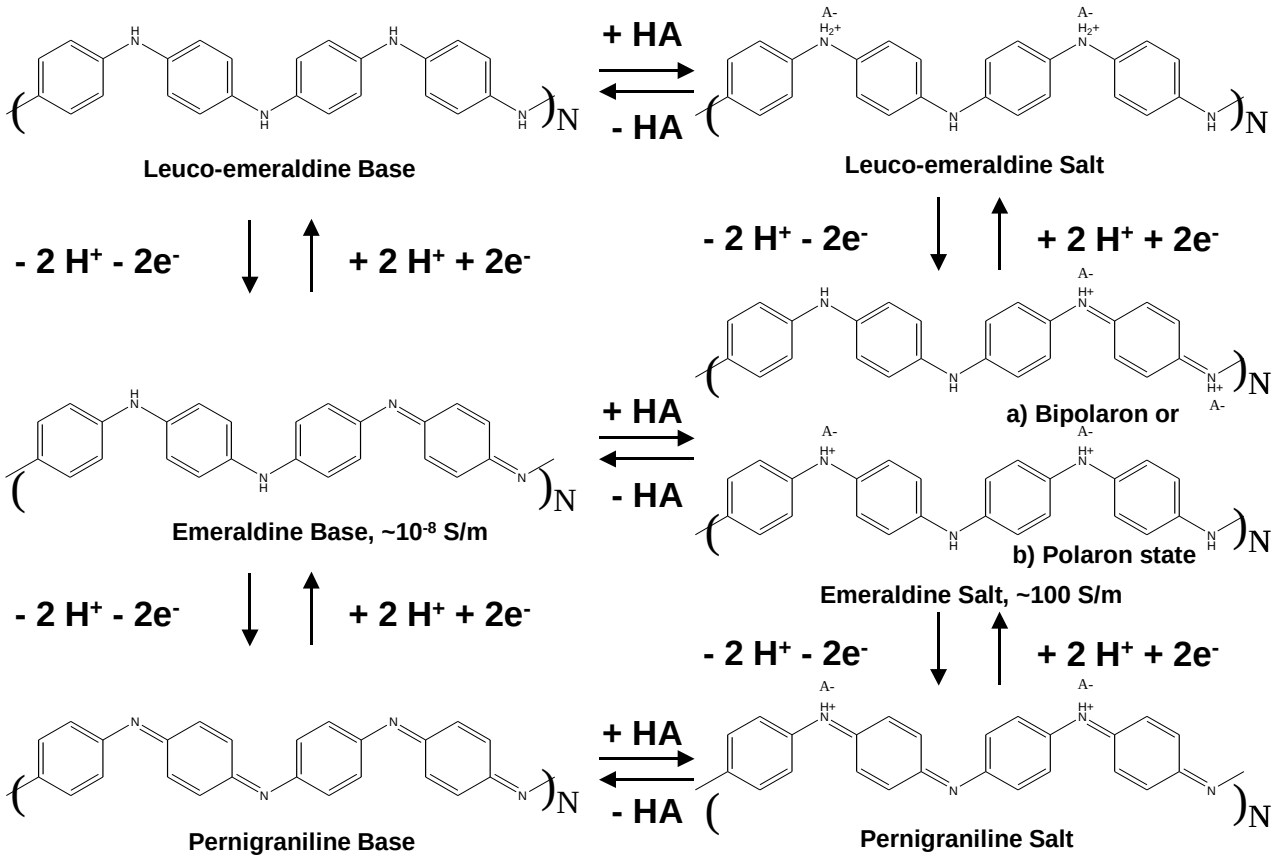

Fig. 1.3 This figure shows the oxidation states of polyaniline [2]. The states of polyaniline are a function of pH (horizontal changes) and electrochemical potential (vertical changes). The oxidation states (vertical) are in fact continuous, leading to a pseudo-capacitive behavior. This figure is referred to section 2.1, in order to show that the polyaniline needs to be protonated for it to enter conductive states. This figure is again referred to in section 2.5 to explain the motivation behind nuclear magnetic resonance tests carried out. Reproduced with permission from the Massachusetts Institute of Technology (copyright holder).

Three main types of materials are commonly studied for supercapacitor applications: (i) carbon, (ii) ruthenium dioxide, and (iii) conducting polymers [3]. However, the energy density of carbon is limited by its specific capacitance of only approximately 100 F/g [4], [5]. Ruthenium dioxide is much more expensive to produce than carbon or conducting polymer materials [3], [4]. Therefore, conducting polymer materials offer a promising avenue of investigation for building new types of supercapacitors. Polyaniline is considered a promising material for supercapacitor applications due to its high specific capacitance, long

cycle life and low production cost [3], [6]. The monomer aniline, from which polyaniline is synthesized, costs only about $6.78 per kilogram [7]. Compared to this, the monomer pyrrole, from which polypyrrole is synthesized, costs about $88.55 per kilogram [8]. The reported specific capacitances are around 150 F/g to 840 F/g [3], [6]. This is well in excess of porous carbon materials at 100 F/g and is close to or in excess of polypyrrole at 170 F/g [9]. The cycle life is expected to be greater than 10^5 cycles [6]. The properties of polyaniline are summarized in Table 1.1 below.

Expected properties	Polyaniline
Specific Capacitance	150-840 F/g [3], [6]
Potential Range	2.88 V to 4.48 V vs. Li/Li^+ [10]
Specific Capacity	67 mAh/g (from above)

Table 1.1 Properties of Polyaniline found in the literature. The specific capacity is estimated at 67 mAh/g based on a specific capacitance of 150 F/g and a 1.6 V voltage range as above.

A lithium titanate electrode is proposed as the counter electrode in this supercapacitor. Lithium titanate is an intercalation compound where ions squeeze into the structure. During this process, the lithium titanate undergoes little appreciable expansion or contraction [11]. This leads to the lithium titanate electrode having a very high cycle life. Lithium titanate electrodes display a battery-like discharge curve, with almost all of the charge transfer occurring very close to 1.5 V vs Li+/Li [11], [12]. Lithium titanate has been found to have long cycle life, high specific capacity and good stability [11]. The expected properties of lithium titanate are summarized in Table 1.2 below.

	Lithium Titanate
Specific Capacity	165mAh/g
Intercalation Potential	1.5V vs. Li/Li+

Table 1.2 Expected Properties of Lithium Titanate [12]

Similar asymmetric hybrid devices have been investigated by combining activated carbon or polyfluorothiophene electrodes with lithium titanate electrodes [11]. Du Pasquier *et al.* note

that such devices would have a voltage of 1.5 V at the end of discharge, as opposed to 0 V for conventional supercapacitors, resulting in a significant increase in energy density. Polyfluorothiophene was used because it is a pseudocapacitive material with a specific capacitance two to three times that of activated carbon [11]. Polyaniline offers promising prospects in conjunction with polyfluorothiophene because it has a higher specific capacity, expected to be around 67 mAh/g as shown in Table 1.1, while polyfluorothiophene only has a specific capacitance of about 40 mAh/g [11] for polyfluorothiophene.

In this thesis, the hybrid supercapacitor/battery (referred to as the "hybrid device" hereafter) suggested is expected to have an energy density comparable to that of some batteries, but with much higher cycle life. If such a device can be built, it can have applications in many areas. As suggested earlier, the device may be used in buoys at sea, where replacements of batteries would be very expensive and energy storage devices with longer lifetimes would be desirable. It may also be useful in a multitude of backup power systems, particularly where battery replacements are difficult. For example, in traffic light backup systems in busy areas, replacing a battery would involve significant disruption to traffic and such replacements should be minimized as far as possible. Some compromise in energy density may be acceptable in exchange for longer lifetimes.

1.5 Outline of Thesis

The aim of this project is to fabricate polyaniline electrodes and test their performance characteristics so as to evaluate their feasibility in combination with lithium titanate electrodes for the hybrid device described above. The purpose of doing so is to create an energy storage device with an energy density rivalling that of batteries, but with much higher cycle life. Chapter 2 of this thesis discusses the growth and performance of the polyaniline. Various methods of growth are surveyed, the methods decided upon are described in detail, the performance of the resulting polyaniline, in terms of specific capacitance and specific capacity, is reported, and the various experimental issues encountered are discussed. Chapter 3 provides a simulation of a full supercapacitor with a polyaniline electrode and a lithium titanate electrode, based on experimentally determined characteristics of each electrode, and

presents the expected hybrid device characteristics, including energy density and cost per kilowatt-hour. Chapter 4 summarizes the conclusions of this thesis.

2 Polyaniline Electrode Growth and Characterization

This chapter discusses the methods of electrode fabrication considered and actually used. It presents the results of these methods and the experimental issues encountered. Cyclic voltammograms are used to measure the specific capacitance and specific capacity of polyaniline. Nuclear magnetic resonance tests of polyaniline at different oxidation states are carried out to determine the concentration of lithium ions present in the polyaniline. This allows the study of the movement of lithium ions in polyaniline as the polyaniline electrode is charged and discharged.

2.1 Methods of Deposition

In this thesis, polyaniline is grown on a conductive substrate. The conductive substrate acts as a current collector and enables swift charge transfer from all parts of the polyaniline to the rest of the circuit. In order to accomplish this, the common procedure used is to electro-deposit polyaniline onto a substrate immersed in a solution containing aniline [3].

Two main methods are described in the literature for the deposition of polyaniline on a substrate – a non-aqueous deposition method and an aqueous deposition method.

In the non-aqueous deposition method, the aniline solution contains no water and uses a non-aqueous solvent such as propylene carbonate or acetonitrile. The advantage of the non-aqueous method is that no water is allowed to come into contact with the polyaniline and there is consequently no need to remove the water from the electrode. The water needs to be removed because the lithium titanate electrode, the other electrode of this supercapacitor, operates in non-aqueous solutions which should not be contaminated by water.

In the aqueous method, which is more commonly used, the aniline solution is deposited onto a substrate from an aqueous and highly acidic solution. Since the solution is aqueous, a strong aqueous acid such as hydrochloric acid or sulphuric acid may be used. The advantage of this method is that the strong acid provides an ample supply of protons which protonate the polyaniline, helping to make it conductive and keep it conductive, as is now discussed.

Fig. 1.2 shows the various states of polyaniline. Polyaniline is conductive when it is in its polaron or bipolaron state [13], that is, in its emeraldine salt state. The figure shows that in order for the polyaniline in its emeraldine base state to become conductive and stay conductive, it needs to be protonated, so that it reaches its polaron or bipolaron state. This is usually done by synthesizing polyaniline in an acidic solution, so as to provide the protons needed to make and keep the polyaniline conductive. Therefore, the aqueous method is more commonly suggested and used [3], [14], [15], [16].

2.2 Three-Electrode Setup

The three-electrode setup is used in this thesis to fabricate the polyaniline electrode and later to test its performance. The basic three electrode setup used in electrochemical experiments is shown in Fig. 2.1 below. The three electrodes of this setup are connected to a potentiostat and used to carry out experiments, as detailed in following sections.

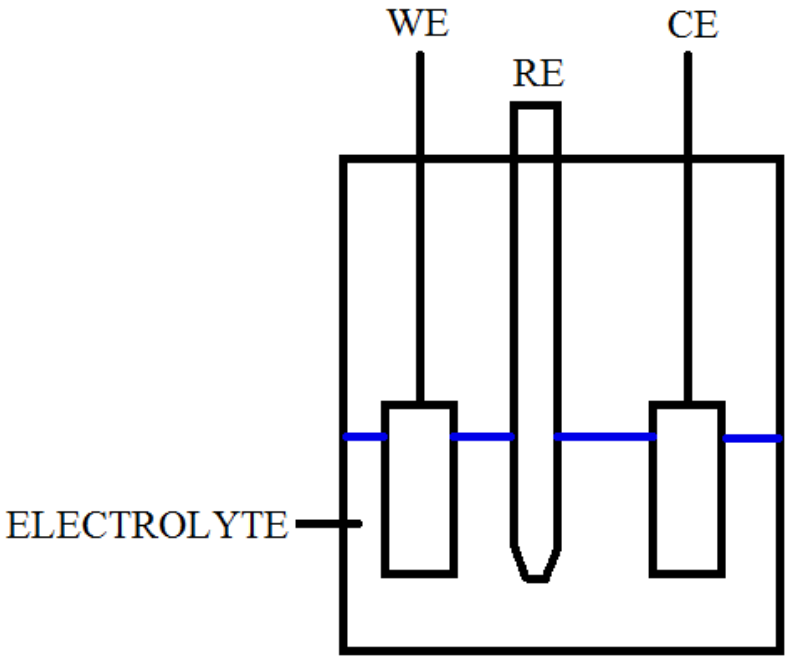

Fig. 2.1 The basic three electrode setup used for electrochemical experiments. WE stands for working electrode, RE stands for reference electrode and CE stands for counter electrode.

The working electrode is the electrode on which polyaniline is grown during the fabrication of the polyaniline electrode. During performance testing, the polyaniline electrode was used as the working electrode. The reference electrode is a special electrode that provides a

constant potential between the electrolyte and the tip of the reference electrode. It can therefore be used as a reference point to measure the potential of the working or counter electrode against. The counter electrode provides a second electrode so that the current in an experiment flows between the working electrode and the counter electrode.

2.3 Non-Aqueous Deposition and Results

Some non-aqueous methods attempted are discussed in this sub-section. As will be seen, this approach did not lead to effective electrodes. The procedure is briefly described nonetheless as a record for future students who may wish to further explore the approach.

2.3.1 Propylene Carbonate

A procedure similar used by Osaka *et al.* [15] was attempted, but with a different substrate and reference electrode. A stainless steel sheet substrate, 3 cm x 1 cm, was used as the working electrode, several sheets of carbon fiber paper stacked together were used as the counter electrode and an Ag/Ag^+ (0.01M $AgNO_3$/acetonitrile) was used as the reference electrode. These were immersed in an electrolyte containing 0.5M aniline (from Sigma Aldrich, St. Louis, MO, ACS reagent, ≥99.5%), 1.0M CF_3COOH (trifluoroacetic acid, ReagentPlus, 99%, obtained from Sigma Aldrich, St. Louis, MO) and 0.5M $LiClO_4$ (lithium perchlorate, ACS reagent, obtained from Sigma Aldrich, St. Louis, MO) in propylene carbonate (ReagentPlus, 99%, obtained from Sigma Aldrich, St. Louis, MO**)**, a non-aqueous solvent. The non-aqueous reference electrode was assembled from a kit ordered from BASi (West Lafayette, IN). The aniline was distilled prior to use. 13 sheets of 3 cm x 3 cm carbon fiber sheets (AvCarb P50, produced by Ballard Material Products, Burnaby, BC, and obtained from Fuel Cell Store online) were stacked together to act as the counter electrode. A constant current density of 0.5 mA/cm^2 is applied between the working and counter electrodes using a Solartron 1287 potentiostat.

According to Osaka *et al.* [15], the deposition of polyaniline is normally done in aqueous solutions so that strong aqueous acids may be used, which provide a plentiful supply of protons to the polyaniline, enabling it to become conductive and allowing the electro-deposition to proceed. Instead of using an aqueous acid, a relatively strong organic acid,

trifluoroacetic acid, is used. Lithium perchlorate is added to the electrolyte to make it more conductive.

However, it was found that the polyaniline deposited using this method had very poor adhesion to the stainless steel. Upon substituting stainless steel with platinum wire, the same problem occurred. The deposited polyaniline could usually be washed off very easily from the substrate.

2.3.2 Acetonitrile

A similar experiment as above was attempted, but using acetonitrile (anhydrous, 99.8%, from Sigma Aldrich, St. Louis, MO) as the solvent. A procedure similar to of Miras *et al.* [10] was used, but using a different substrate and reference electrode. The same electrodes as above were immersed in a solution containing 0.1M aniline and 0.5M $LiClO_4$ in acetonitrile. The working electrode's potential was cycled between -0.5 V and 1 V at 50 mV/s for a few cycles. Miras *et al.* [10] suggest that an acid is not necessary because acetonitrile is a protophobic solvent and therefore protons released during aniline oxidation are sufficient for the reaction to take place.

However, upon attempting this experiment, the polyaniline once again had very poor adhesion to the stainless steel substrate. The polyaniline could be seen falling off the substrate as the deposition took place.

The likely reason for the failure of deposition from non-aqueous electrolytes is that the polyaniline was not sufficiently protonated, since strong acids cannot be used in non-aqueous electrolytes, and therefore the electro-deposition reaction was impeded.

2.4 Aqueous Deposition

The aqueous deposition method used is discussed in this sub-section.

2.4.1 Introduction and Review of Methods

In the aqueous deposition method, as explained above, strong aqueous acids are typically used in water along with aniline. Some of the common deposition techniques are reviewed below.

There is a choice between using potentiostatic, galvanostatic and potentiodynamic deposition methods. In the potentiostatic method, a constant potential is applied between the working electrode and the reference electrode for a period of time. In the galvanostatic deposition method, a constant current is applied between the working electrode and the counter electrode for a period of time. In the potentiodynamic method, the potential of the working electrode (with respect to the reference electrode) is swept back and forth across a potential range at a fixed rate for a certain number of cycles.

Of these methods, the potentiodynamic method is considered to be superior for the reasons given by Mondal *et al.* [17]. In the potentiodynamic method, at fast sweep rates, the polyaniline is deposited in thin layers, adding to its porosity. Also, in the potentiodynamic method, the polymerization of polyaniline is regularly interrupted between consecutive sweeps, giving time for intermediates to escape from the polyaniline. This results in polyaniline of greater purity. In the potentiodynamic method, the polyaniline is deposited in fine layers, and each layer is electrochemically activated before the next layer is deposited. This leads to greater porosity and minimizes any intermediates (impurities) that may be trapped in clusters of polyaniline in the other methods.

2.4.2 Deposition of Polyaniline

Using the three-electrode setup described earlier, polyaniline was deposited onto a stainless steel sheet substrate. A 3 cm x 1 cm stainless steel substrate was used as the working electrode, and 13 sheets of 3 cm x 3 cm carbon fiber sheets (AvCarb P50, produced by Ballard Material Products, Burnaby, BC and obtained from Fuel Cell Store online) were stacked together to act as the counter electrode. This is done in order to ensure that the surface area of the counter electrode greatly exceeds that of the working electrode, so that the counter electrode does not limit the current. If the counter electrodes are not large enough to

handle the current drawn by the working electrode, they degrade quickly. These electrodes were immersed to a depth of 2 cm in an electrolyte solution consisting of 0.5M aniline and 0.5M H_2SO_4 in water. The stainless steel electrodes were polished with sandpaper and cleaned with acetone and water prior to use. The aniline was distilled prior to use to remove any impurities present. De-ionized water was used so as to minimize impurities in the water.

The potential of the working electrode was swept between -0.235V and 1.165V vs. an Ag/AgCl reference electrode (obtained from BASi, West Lafayette, IN) at a rate of 200 mV/s. As before, the Solartron 1287 was used and the aniline was distilled prior to use. 227 deposition cycles were done over approximately an hour. Fig 2.2 below shows the current vs. working electrode potential as the growth occurs. The increase in current with each sweep shows that polyaniline is being deposited on each sweep. This is because as more polyaniline is deposited on the electrode, it becomes more capacitive, and the current flowing through a capacitor is directly proportional to its capacitance. Therefore, a higher capacitance, caused by a greater amount of polyaniline, leads to a higher current.

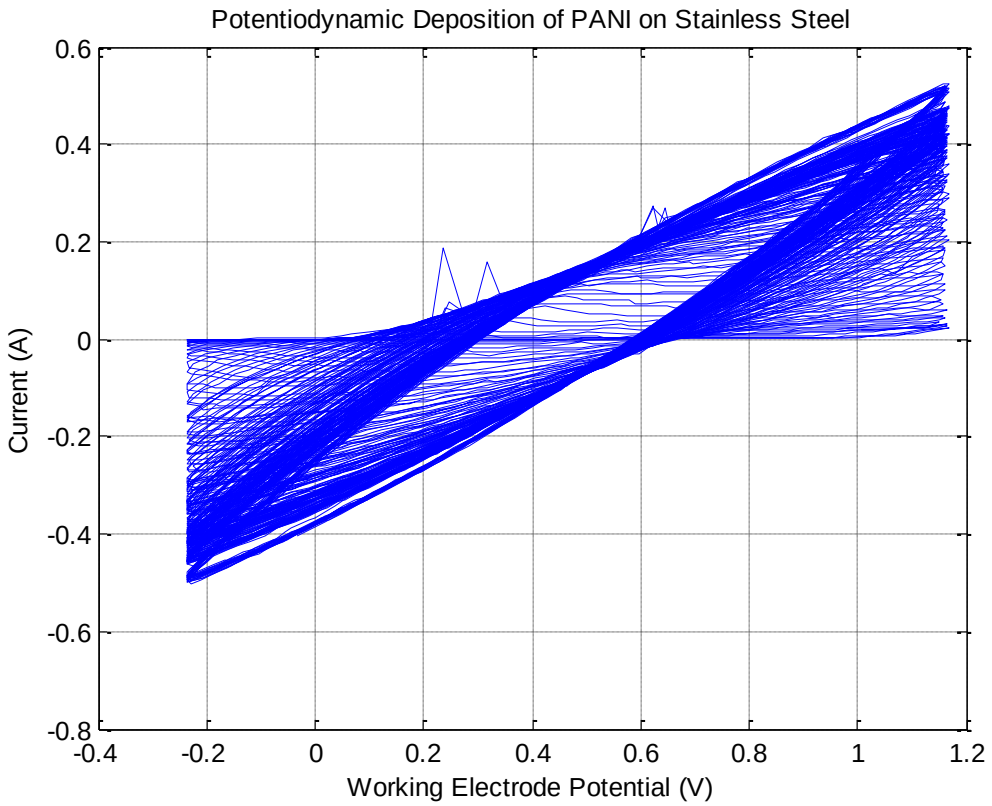

Fig. 2.2 Current vs. working electrode potential during deposition. The current increases with each sweep, showing that polyaniline is being added to the substrate. The voltage shown is measured against an Ag/AgCl reference electrode and a scan rate of 200 mV/s is used. The direction of cycling is clockwise.

After this, the polyaniline was quickly removed from the electrolyte and placed in 500 mL of de-ionized water and left overnight. This allowed any intermediates or impurities, as well as the acid, to be leached out of the polyaniline. The carbon fiber papers (forming the counter electrode) were also soaked in water in a similar manner. Then, the polyaniline was dried in an oven at 67ºC for approximately 30 minutes, in order to remove the water.

2.4.3 Testing of Polyaniline Performance

In this section the polyaniline is tested in order to measure its specific capacitance (F/g) and specific capacity (mAh/g). The specific capacitance is the capacitance of the polyaniline per unit mass, while the specific capacity is the amount of charge that can be stored per unit mass. The capacitance of the polyaniline electrode is measured using a technique known as

cyclic voltammetry. In this technique, the polyaniline electrode is cycled back and forth across a voltage range at a specified sweep rate (mV/s). Since for an ideal capacitor

$$i = C\frac{dV}{dt},$$

the current generated is proportional to the rate of change of voltage (dV/dt), the amount of current generated allows the measurement of capacitance. If the polyaniline electrode is behaving capacitively, the current vs. voltage graph in the cyclic voltammogram should look roughly rectangular. This is because in a pure capacitor, the current is constant at a certain value when dV/dt is positive, and when dV/dt is reversed, the same current flows in the opposite (i.e. negative) direction. By integrating the current over time, the amount of charge entering or leaving polyaniline may be estimated. From this, the specific capacity (i.e. amount of charge stored by a certain amount of polyaniline) can be estimated.

The polyaniline electrode was immersed as the working electrode in a non-aqueous solution containing 0.5M $LiClO_4$ in acetonitrile. This electrolyte is used as it is appropriate for use with lithium titanate in the battery/supercapacitor configuration, due to the presence of Li^+ ions. The acetonitrile was bubbled with nitrogen before use. Carbon fiber papers, as before, were used as the counter electrode. An $Ag/AgNO_3$ reference electrode was used. A cyclic voltammogram was carried out where the polyaniline electrode was cycled between -0.350 V and 0.950 V at a rate of 1 mV/s for 3 cycles. The result is shown in the Fig 2.3 below.

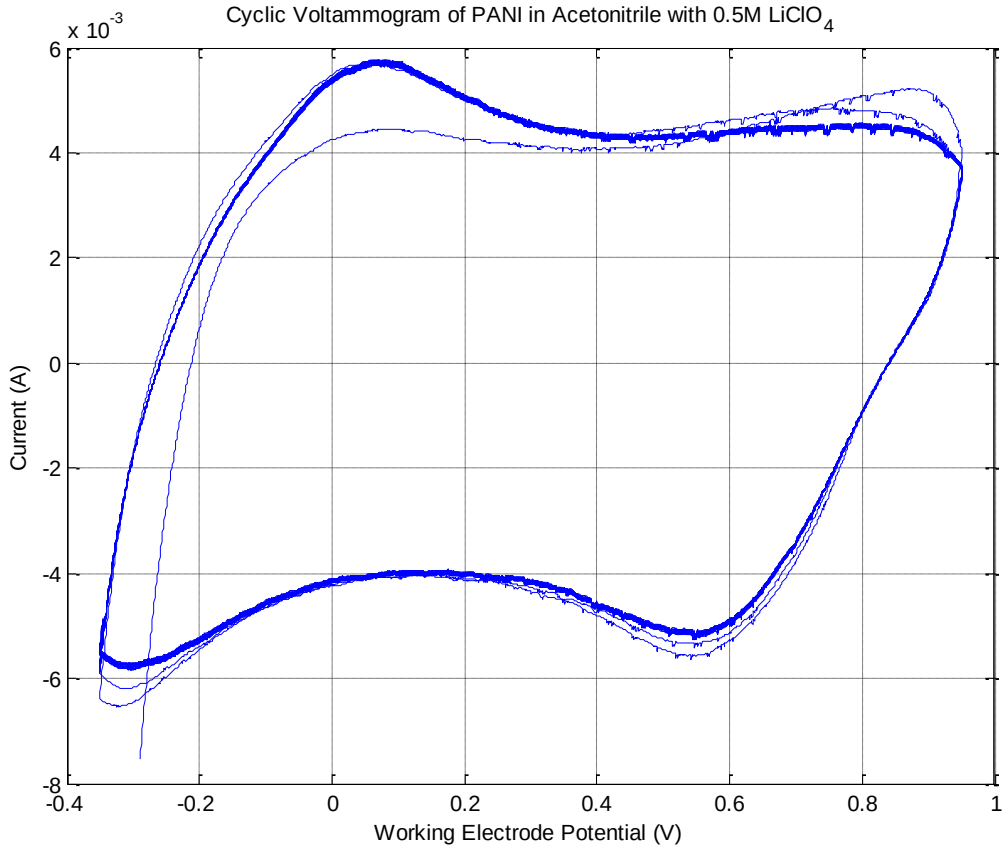

Fig. 2.3 Cyclic voltammogram of polyaniline electrode in acetonitrile with 0.5M $LiClO_4$. The voltage shown is measured against an $Ag/AgNO_3$ reference electrode and a scan rate of 1 mV/s is used. The direction of cycling is clockwise. 23 cycles are shown.

The peaks in the above graph show the transitions in state. When oxidizing (i.e. increasing voltage), peaks are seen just above 0 V and just past 0.8 V. The first peak is likely the transition from a leuco-emeraldine state to a polaron state, when the polyaniline becomes very conductive. The second peak is likely the transition from a polaron state to a bipolaron state, which is also conductive [13]. The same peaks are observed when reducing, at slightly lower potentials. The above potential range was picked to keep the polyaniline in its conductive states and to prevent over-oxidation. This is explained further in section 2.4.4.2. From the above cyclic voltammogram, the capacitance of the electrode can be estimated using the formula

$$i = \frac{d(CV)}{dt} \approx C\frac{dV}{dt}.$$

Although the capacitance changes slightly with the potential of the electrode, this variation is ignored for the purpose of calculating specific capacitance. The current i can be estimated by taking the current in each direction, measured at roughly the middle of the potential range. dV/dt is equal to the cycling rate. In the figure above, the current in either direction, on average, is approximately 4.4 mA, at the midpoint of the potential range (i.e. 0.3V). The cycling rate is 1 mV/s. Therefore, the capacitance of the above electrode is approximately 4.4 farads. The mass of the polyaniline on the electrode is 19.8 mg (found by weighing the electrode before and after the deposition and taking the difference). Therefore, the specific capacitance of the polyaniline is found to be about 220 F/g. This roughly agrees with the specific capacitance of 150 F/g reported in Fusalba *et al.* [6]. A specific capacitance of only 107 F/g is reported by Ryu *et al.* [18], but the specific capacitance in the above experiment is likely higher because a high scan rate is used, leading to fine layers and greater porosity in the polyaniline. A higher specific capacitance of 380 F/g is reported by Park and Park [19], but the method involved adding other materials (namely, conducting powder and polytetrafluroethylene) to the polyaniline and not including their mass in the specific capacitance.

By integrating the current over time, the amount of charge entering or leaving polyaniline may be estimated. Based on this, the specific capacity is estimated to be 85 mAh/g. This is a measure of how much charge the polyaniline can hold, and will be critical in determining the overall energy density of the hybrid device.

Since the above CV shows 23 cycles, and the capacitance of the polyaniline appears to be fairly stable, we can be reasonably certain that the above capacitance and capacity figures are realistic estimates. A detailed study of polyaniline lifetime is beyond the scope of this thesis since it would involve testing the polyaniline over several thousands of cycles, a process that would take thousands of hours. Moreover, if these polyaniline electrodes were to be commercially produced, they would likely be produced in even more pure conditions, which

could further increase lifetime. For example, the entire experiment, including deposition, could be done under an inert atmosphere to prevent any degradation. While it is not clear whether this would improve the polyaniline electrode's characteristics, Asturias and Macdiarmid [20] note that growing polyaniline under inert atmosphere instead of air has some impact on the polyaniline oxidation state, and as a precaution Macdiarmid *et al.* assembled electrodes under an inert atmosphere [21]. The materials used could also be subjected to even more thorough and time-consuming purification steps.

The entire experiment described above was repeated, and the specific capacitance and specific capacity figures obtained were similar (within about 5%).

2.4.4 Experimental Issues

Several experimental issues were encountered while attempting the deposition of polyaniline and they are described in the sub-sections below.

2.4.4.1 Importance of Soaking Electrodes after Deposition

It was observed that if the polyaniline electrode is not soaked in water soon after the deposition, the capacitance tends to die off within a day or less. This is most probably because the acidic electrolyte left over in the electrode from deposition reacts with the polyaniline and causes it to degrade. The problem was solved by soaking the polyaniline electrode in de-ionized water for at least 24 hours. This technique of soaking the electrode in water follows the methods of Raj *et al.* [14].

2.4.4.2 Finding the Appropriate Voltage Range for Performance Testing

In order to find the appropriate working electrode voltage range to cycle the polyaniline electrode for performance testing, without damaging the electrode, tests were carried out which pushed the voltage to extremes in both directions. The aim was to find the voltage range in which the polyaniline electrode behaves like a capacitor. The results are presented below.

When the voltage was set to be between 0 V and 1.4 V, the cyclic voltammogram in Fig. 2.4 below was obtained.

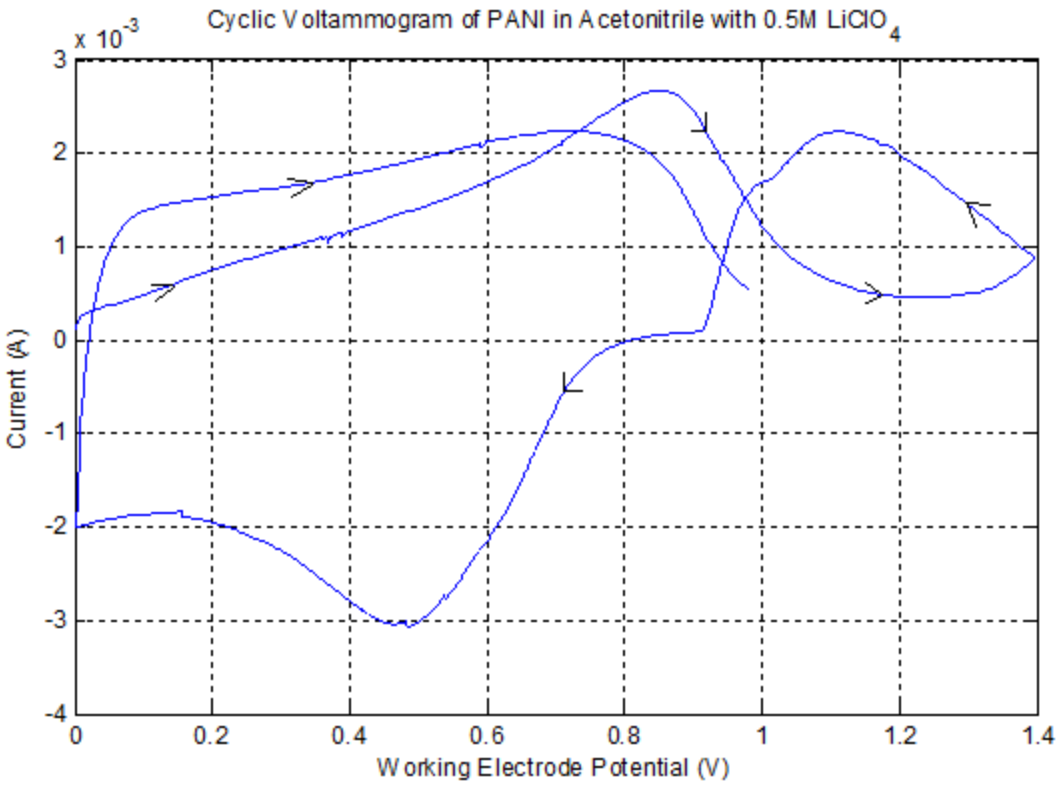

Fig. 2.4 Cyclic voltammogram of polyaniline in acetonitrile with 0.5M $LiClO_4$ to test the upper limit of the polyaniline electrode's potential. The voltage shown is measured against an $Ag/AgNO_3$ reference electrode and a scan rate of 1 mV/s is used. The direction of cycling is clockwise.

In the above figure, a fishtail pattern was obtained when the working electrode potential was pushed above 0.950 V, indicating possible degradation of the electrode. The exact reasons behind the degradation are unclear, but it was decided not to go beyond 0.950 V since the electrode is not behaving capacitively in that region. Similar patterns are observed by Tang *et al.* [22] when over-oxidizing polyaniline. Therefore, the upper limit for cyclic voltammograms was set to be 0.950 V.

The lower voltage limit was investigated by pushing it down to -0.7 V. Fig. 2.5 below shows the result.

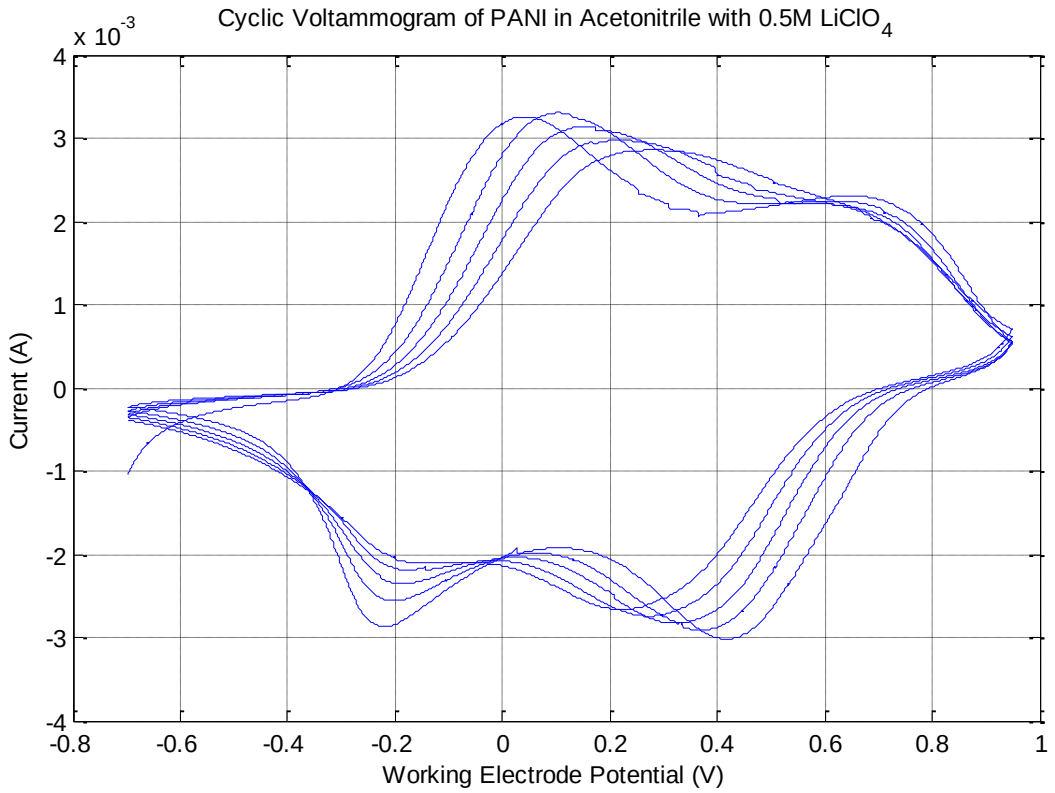

Fig. 2.5 Cyclic voltammogram of polyaniline in acetonitrile with 0.5M $LiClO_4$ to test the lower limit of the polyaniline electrode's potential. The voltage shown is measured against an $Ag/AgNO_3$ reference electrode and a scan rate of 1 mV/s is used. The direction of cycling is clockwise.

The figure above shows that below approximately -0.350 V, the current tends to taper off. Since there is not a large amount of current below this potential, such low potentials are not used. The tapering off in current at low potentials is consistent with the work of others [10], [16]. It is likely that the first peak, observed just above 0 V when oxidizing and just below -0.2 V when reducing in the above figure, is the transition point at which the polyaniline is converted to or from its leuco-emeraldine state to its polaron state. Polyaniline has low conductivity in its leuco-emeraldine state but is conductive in its polaron state. This is the likely reason why the current tapers off to the left of this peak. Therefore, the lower limit for cyclic voltammograms was determined to be -0.350 V.

2.4.4.3 Comments on Different Scan Rates

In order to find an appropriate scan rate for testing the polyaniline electrode in a cyclic voltammetry experiment, a number of different scan rates were tried. Faster scan rates allow tests to be done more quickly, but may not provide enough time to allow for the diffusion of ions into the polyaniline electrode. Therefore, the scan rates need to be slow enough to allow fully for ion diffusion and charge transfer.

The results from cycling the polyaniline electrode at 20 mV/s, 10 mV/s, 5 mV/s, 1 mV/s and 0.1 mV/s are shown in Fig. 2.6 below. Since the current is proportional to the scan rate in a pure capacitor, the capacitive portion of the current is higher at higher scan rates. In order to compensate for this, the current divided by the scan rate is presented on the vertical axis. This is referred to as the normalized current.

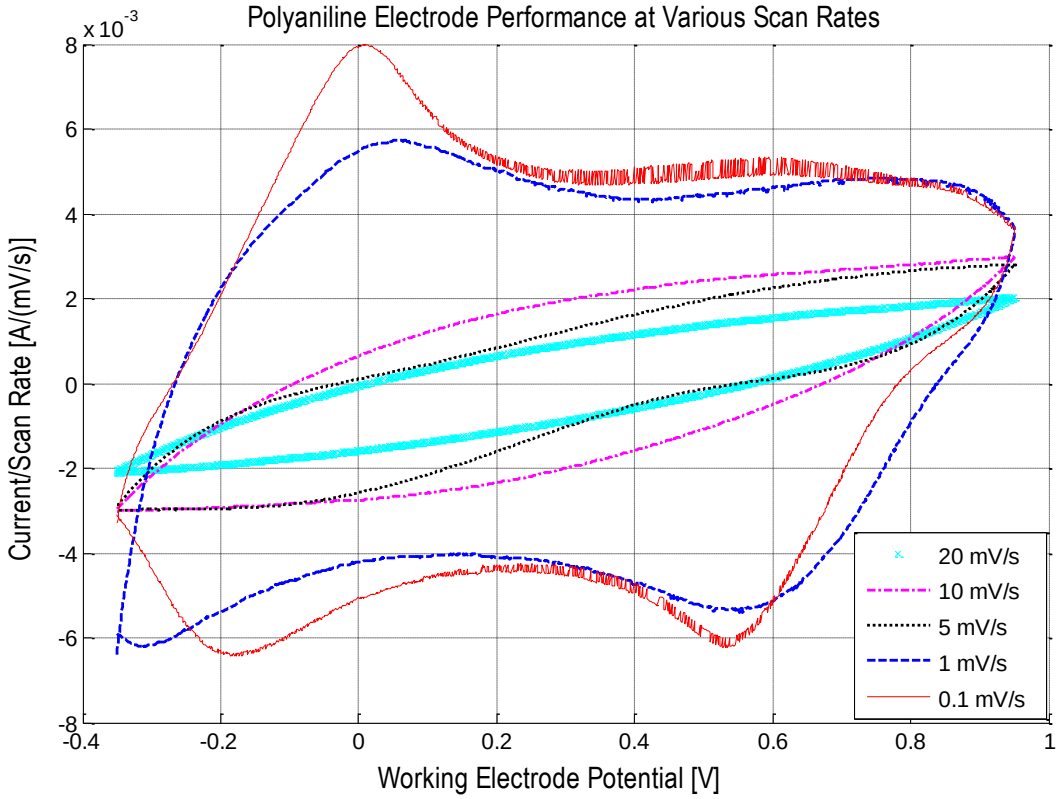

Fig. 2.6 Results of cycling the polyaniline electrode at various scan rates. The vertical axis is the current divided by the scan rate (normalized current), making it possible to compare cyclic voltammograms from different scan rates. The voltage shown is measured against an $Ag/AgNO_3$ reference electrode. The direction of cycling is clockwise.

The figure above shows that 20 mV/s, 10 mV/s and 5 mV/s all appear to be too fast to allow for diffusion of ions into the electrode the electrode. This is why the normalized currents at these scan rates appear to be lower than the normalized current at 1 mV/s or slower. Also, the shapes of these graphs show that the current does not appear to saturate at any level.

On the other hand the normalized currents appear to roughly similar at 1 mV/s and 0.1 mV/s. The peaks are more pronounced and visible at 0.1 mV/s, but the overall rectangular shape, and therefore the value of capacitance obtained, is roughly the same. Therefore, 1 mV/s appears to be an appropriate rate to scan the electrode.

2.4.4.4 Importance of Using Counter Electrode with Sufficient Surface Area

The experiments above were conducted with 13 sheets of carbon fiber, each with 2 cm x 3 cm immersed in solution, even though the stainless steel substrate only had 2 cm x 1 cm immersed in solution. It was important to ensure that the counter electrode's surface area was much greater than that of the working electrode. This is because if the counter electrode does not have a relatively large surface area, its capacitance tends to be low. Therefore, when charge is passed through the counter electrode, the voltage across the electrochemical double layers formed in the carbon tends to be high, and this may cause degradation reactions to take place. If the carbon fiber disintegrates during an experiment, the carbon particles may coat the polyaniline electrode and limit its capacitance.

By using several sheets of carbon fiber paper stacked together, the capacitance of the counter electrode is greatly increased and the voltage across the double layers in the carbon drops, thereby avoiding the degradation reactions. In fact, the above experiments (both deposition and performance testing) were initially done with only 1 sheet of carbon fiber paper instead of 13. However, when such experiments were done, the carbon fiber paper disintegrated after a few cycles and the cyclic voltammograms did not appear very capacitive.

2.5 NMR Tests

In the battery-supercapacitor combination described above, since a lithium titanate electrode is used, it would be beneficial if the polyaniline could absorb Li^+ and be doped by these ions,

instead of protons. This is because the lithium titanate electrode, being a lithium intercalaction compound, will emit large amounts of lithium ions into the solution, and if the polyaniline can store some of those lithium ions, then less electrolyte would be needed to keep those ions from precipitating out.

Nuclear magnetic resonance (NMR) tests were carried out in order to determine whether the lithium levels in the polyaniline changed with potential. If so, this would indicate that the change of polyaniline state was being driven by lithium doping and that the lithium ions are indeed being stored in the polyaniline. Therefore, two samples were grown, one set to −0.350 V and the other to 0.950 V vs. an $Ag/AgNO_3$ reference electrode. It was expected that if the lithium does dope the polyaniline, then the concentration of lithium ions would vary greatly between the two samples, since the lithium ions would move in and out of the polyaniline. Referring back to Fig. 1.2, it can be seen that the movement of protons in and out of polyaniline cause transitions in the polyaniline state. It was speculated that perhaps the lithium ions (Li^+), if they doped the polyaniline, could play the role of protons in Fig. 1.2, since protons are not explicitly introduced through acids. If so, the difference in lithium ion concentration between the two samples should roughly equal the amount of charge transfer needed to move the polyaniline from one state to the other.

Another direction of research that could be pursued in this area would be to try and grow the polyaniline with anions embedded in them. If this can be done, then a large number of lithium ions would be stored in the polyaniline to balance the anion charge.

In the NMR spectroscopy, the sample is placed under a magnetic field. Certain nuclei, including the dominant isotope of lithium, absorb and re-emit this electromagnetic energy, at resonant frequencies determined by the nature of the nuclei. Therefore, by placing samples with lithium ions under NMR testing, the relative intensity of the resonant peak formed is proportional to the amount of lithium ions in the sample. This principle is used to measure the quantity of lithium ions in polyaniline samples at different oxidation states.

The amount of charge transfer expected from the NMR tests, if the lithium does dope the polyaniline, is calculated below. The results from two samples of polyaniline, both at an initial potential of approximately -0.130 V, are considered. The potential of one sample was set to -0.350 V and the potential of the other was set to 0.950 V (vs. $Ag/AgNO_3$). In each case, the charge transfer needed was measured. The results are presented in Table 2.1 below.

Final Potential (V)	Mass of Sample (mg)	Charge Transfer (C)
-0.350	7.5	1.95
0.950	10.5	0.17

Table 2.1 Charge transfer while setting potential to desired values.

Linearly adjusting the above values to those expected from a 23.3 mg sample (this was the mass of the sample used in the actual NMR experiment), the results in Table 2.2 are obtained.

Potential (V)	Charge Transfer (C)
-0.350 V	6.06
0.950 V	0.38
Overall Charge Transfer	6.44

Table 2.2 Charge transfer to go between states for 23.3 mg sample of polyaniline

The above calculations show that if the lithium is doping the polyaniline and causing the charge transfer, then 6.44 C of charge transfer may be expected. This is converted to millimoles of lithium ions below:

$$\frac{6.44\ C}{1.6\times10^{-19}\ C/\ Li^{+}\ ion}\times\frac{1\ mol}{6.02\times10^{23}\ Li^{+}\ ions}\times\frac{1000\ mmol}{1\ mol}=0.0670\ mmol\ of\ \ Li^{+}\ ions\,.$$

Therefore, a change of 0.0670 mmol of lithium ions are expected in the NMR tests, based on the charge transfer from the -0.350 V state to the 0.950 V state. If the change in lithium ions from the NMR tests is significantly less, then the lithium ions are not responsible for the charge transfer.

The samples for the NMR tests were created by growing polyaniline on stainless steel substrates according to the procedure described in thesis, setting them to the desired potential and then scraping off the polyaniline with a blade and putting it into small tubes, with an inner diameter of 4.2 mm and a length of approximately 4 cm, suitable for the NMR tests. Each tube was about 70% full of polyaniline. Each sample was scanned eight times and the average readings are presented in Table 2.3 below.

The results are presented in the table below.

Potential (V)	Mass of Sample (mg)	Relative Intensity
-0.350	23.3	2212/scan
0.950	31.9	3849/scan

Table 2.3 Results from NMR Tests. The relative intensities are accurate within approximately 2%, assuming that all of each sample is located within the sensitive region of the coil of the NMR spectrometer when the measurement is carried out.

A standard solution of lithium chloride, with a known quantity of lithium ions, was tested so that a basis of comparison is obtained to convert the above values into quantities of lithium ions. This standard solution yielded a relative intensity reading of 3890 per scan, and it contained 1.40 mg of LiCl. The relative intensity readings obtained in the NMR tests are directly proportional to the amount of lithium ions in the sample. Therefore, if a sample with a known quantity of lithium ions is tested, its relative intensity reading can be used as a basis to calculate the amount of lithium ions in other samples from their relative intensity measurements.

Based on the above results, the quantity of lithium in each of the polyaniline samples above can be calculated, as shown below.

For the -0.350 V sample:

$$\frac{2212.3}{3890} \times 1.40\ mg \times \frac{1 mol}{42.394\, g} = 0.0188\, mmol\ Li^{+} \quad .$$

For the 0.950 V sample:

$$\frac{3849.8}{3890} \times 1.40\ mg \times \frac{1 mol}{42.394\, g} = 0.0327\, mmol\ Li^{+} \quad .$$

In order to compare the two readings, they must be adjusted for mass. If the 0.950 V sample weighed only 23.3 mg, as with the -0.350 V sample, then it would contain 0.0239 mmol Li^{+} (by mass proportion):

$$0.0327\, mmol \times \frac{23.3\, mg}{31.9\, mg} = 0.0239\ mmol\ Li^{+} .$$

Therefore, the change in lithium ion concentration between the two samples, normalized to the smaller sample, is given by:

0.02387 mmol – 0.01878 mmol = **0.00509 mmol Li^{+}.**

Therefore, the NMR tests show that a change of 0.00509 mmol of lithium ions occurs in a sample of polyaniline of mass 23.3 mg when it is shifted from -0.350 V to 0.950 V (vs. $Ag/AgNO_3$ reference).

Compared to the value expected earlier, 0.067 mmol of lithium ions, the actual difference in lithium ion concentration between the samples is low, less than 8% of what was expected. Therefore, the conclusion is that the charge transfer in the polyaniline is not driven by the lithium ions doping the polyaniline. When lithium ions are emitted by the lithium titanate electrode, there is no expectation that they will be absorbed into the polyaniline in order to

change the polyaniline potential. The electrolyte must therefore be sufficiently large in volume to accommodate all the lithium ions emitted by the lithium titanate electrode, a consideration that could reduce the overall energy density of the electrochemical storage device. The quantity of electrolyte required will be discussed in Chapter 3 of this thesis.

2.6 Concluding Remarks

Based on the tests described in this chapter, the polyaniline is found to have a specific capacitance of approximately 220 F/g and a specific capacity of around 85 mAh/g. Based on the NMR tests described, it has been shown that the lithium ions do not dope the polyaniline and account for the change in its oxidation state. In the following chapter, the full hybrid device is simulated based on the data for each constituent electrode. Since the polyaniline is found not to store lithium ions, allowance must be made for the electrolyte to hold all the lithium ions coming from the lithium titanate electrode during charge transfer.

3 Estimated Performance of the Full Hybrid Device

In this chapter, the combined performance of the polyaniline electrode with a lithium titanate electrode in a full supercapacitor is estimated, based on the results obtained so far for polyaniline and lithium titanate. Unfortunately the full hybrid device could not be built and tested because the lithium titanate degraded very quickly and came off the stainless steel substrate it was deposited on. This issue needs to be investigated in greater detail. However, data was available from testing each electrode independently and this data was combined in a Matlab simulation to estimate the properties of the hybrid device.

3.1 Simulation Method

A simulation is carried out, based on available experimental results from testing each electrode independently, where the full hybrid device is charged with a constant current and discharged with a constant current of the same magnitude.

As the charge transfer proceeds, the voltage of the polyaniline may be estimated based on the data obtained from its cyclic voltammogram. If current is integrated over time, the cyclic voltammogram shows the potential of polyaniline at various states of charge. This data is used to estimate the voltage of polyaniline as it is charged or discharged with a constant current. The voltage is converted and expressed against a lithium reference electrode, in order to enable comparison with the lithium titanate electrode potential (which is usually measured against lithium as a reference). In order to do this, the relative potential between the $Ag/AgNO_3$ reference electrode and a lithium reference electrode was measured and the $Ag/AgNO_3$ reference electrode was found to be 3.05 V vs. the lithium reference electrode. The polyaniline data presented in Chapter 2 was used.

As for the lithium titanate electrode, its potential remains stable at 1.58 V throughout much of the charging process and at 1.54 V throughout much of the discharging process. Lithium titanate tends to maintain a constant potential throughout a charging or discharging cycle, except at the very end of such a cycle when there is a spike in potential. This is shown in Fig. 3.2. This electrode was fabricated and tested by myself, and fellow students Eddie Fok

and Niloofar Fekri. The electrode construction approach, test cell and procedure were devised by Eddie Fok. The work to fabricate and characterize the particular electrodes whose results are used in this thesis was shared equally between us. The lithium titanate electrode was placed in a Swagelok cell with a lithium foil as counter electrode and another lithium piece for the reference electrode. The lithium used was lithium ribbon of thickness 0.38 mm and of 99.9% trace metals basis (supplied by Sigma Aldrich, St. Louis, MO). A small piece of lithium foil, about 1 cm x 0.5 cm was cut out for use as the reference electrode. The lithium foil counter electrode was made as large as possible, so that it did not impede the flow of current. A diagram of the Swagelok cell setup is shown in Fig. 3.1 below.

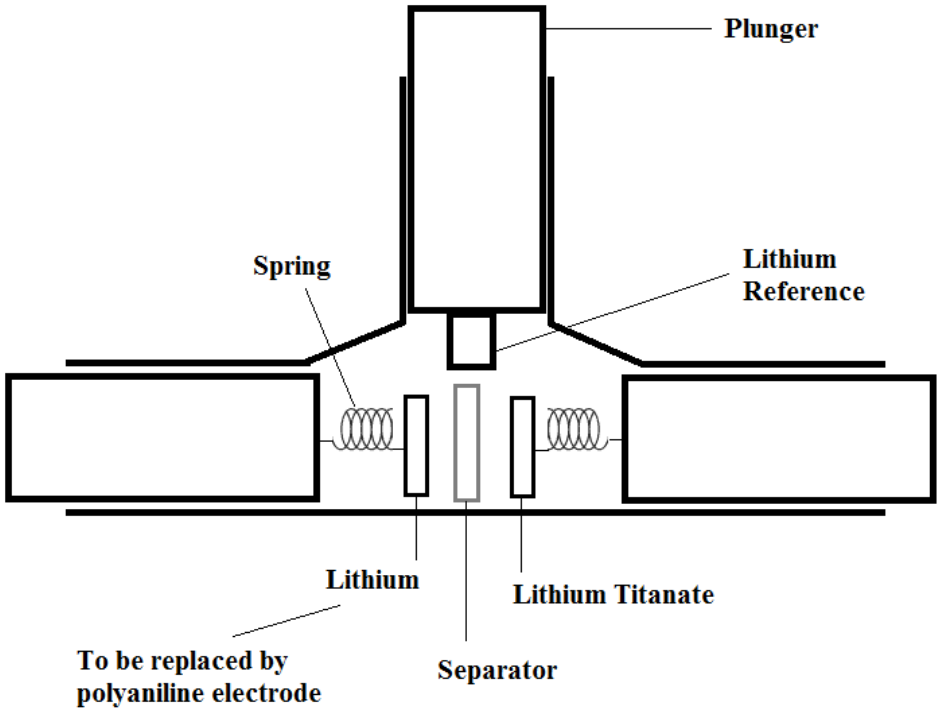

Fig. 3.1 Diagram of Swagelok cell used to assemble hybrid device. The two electrodes, working and counter, are each attached to a plunger with a spring. These springs push the electrodes towards the separator inside the cell. The cell is filled with electrolyte and another plunger with a lithium reference electrode attached is lowered into the electrolyte. As noted on the diagram, lithium was used for the counter electrode as well, in order to test the performance of lithium titanate on its own. However, this will be replaced by the polyaniline electrode at a later stage to form the complete hybrid device. This test cell was designed and built by Eddie Fok.

The lithium titanate was charged and discharged and the results are shown in Fig. 3.2. As mentioned above, its potential is found to be stable over time at 1.58V during charging and 1.54 V during discharging, versus a lithium reference electrode.

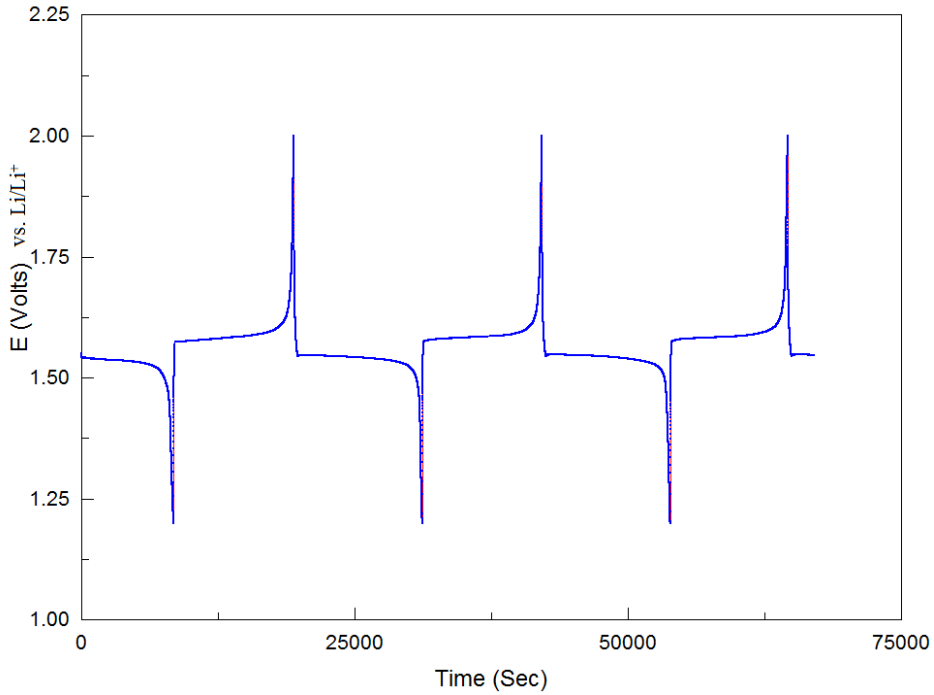

Fig. 3.2 Voltage of lithium titanate during charge-discharge cycles, against a lithium reference electrode. The potential is stable over time at 1.58 V during charging and 1.54 V during discharging. The potential spikes only near the very end of a charging or discharging cycle, but remains almost constant at other times.

The cell simulated in this chapter uses a polyaniline sample weighing 19.8 mg deposited on a 2 cm x 1 cm stainless substrate. As noted before, the polyaniline has a specific capacity of 85 mAh/g. Since the lithium titanate electrode has a specific capacity of 165 mAh/g, the ratio of polyaniline to lithium titanate should be 165:85, so that the charge storage on each electrode is matched. This ratio reduced to 1.94:1 and therefore 10.2 mg of lithium titanate is required.

The cell simulated is shown in Fig. 3.3 below.

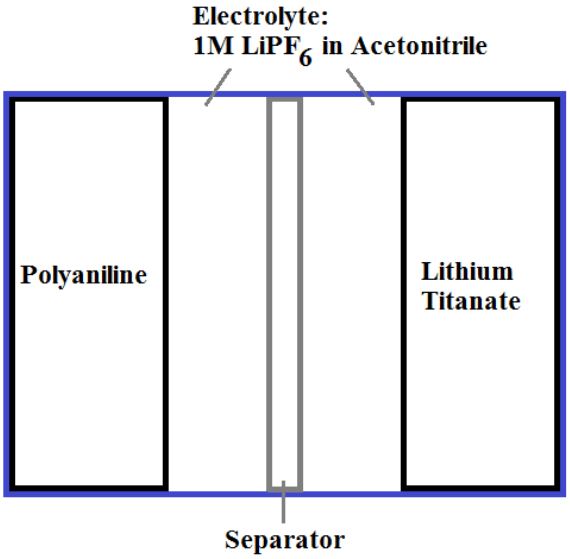

Fig. 3.3 Diagram of the energy storage cell being simulated. The device being simulated comprises of a polyaniline electrode weighing 19.8 mg and a lithium titanate electrode weighing 10.2 mg. A separator is placed between them so that any mechanical deformations that may occur do not cause the two electrodes to touch each other and electrically short out. The electrolyte used is 1M $LiPF_6$ in acetonitrile. The use of 1M $LiPF_6$ is common in such applications, as is explained below.

As explained above, the cyclic voltammetry data for the polyaniline is used to estimate the voltage of the polyaniline, versus lithium reference, for any given state of charge. The voltage of the lithium titanate is assumed to be 1.58 V on charging and 1.54 V on discharging, versus lithium reference. Therefore, the difference between the polyaniline electrode and the lithium titanate electrode potentials (versus lithium reference) is the two-terminal voltage of the supercapacitor.

The Matlab script used to carry out this simulation is included in Appendix A.

3.2 Results of Simulation

Using the methods described above, the two-terminal voltage of the hybrid device was simulated for a constant current charging cycle and a constant current discharging cycle. Fig. 3.4 below shows the change in the two-terminal voltage as this is done.

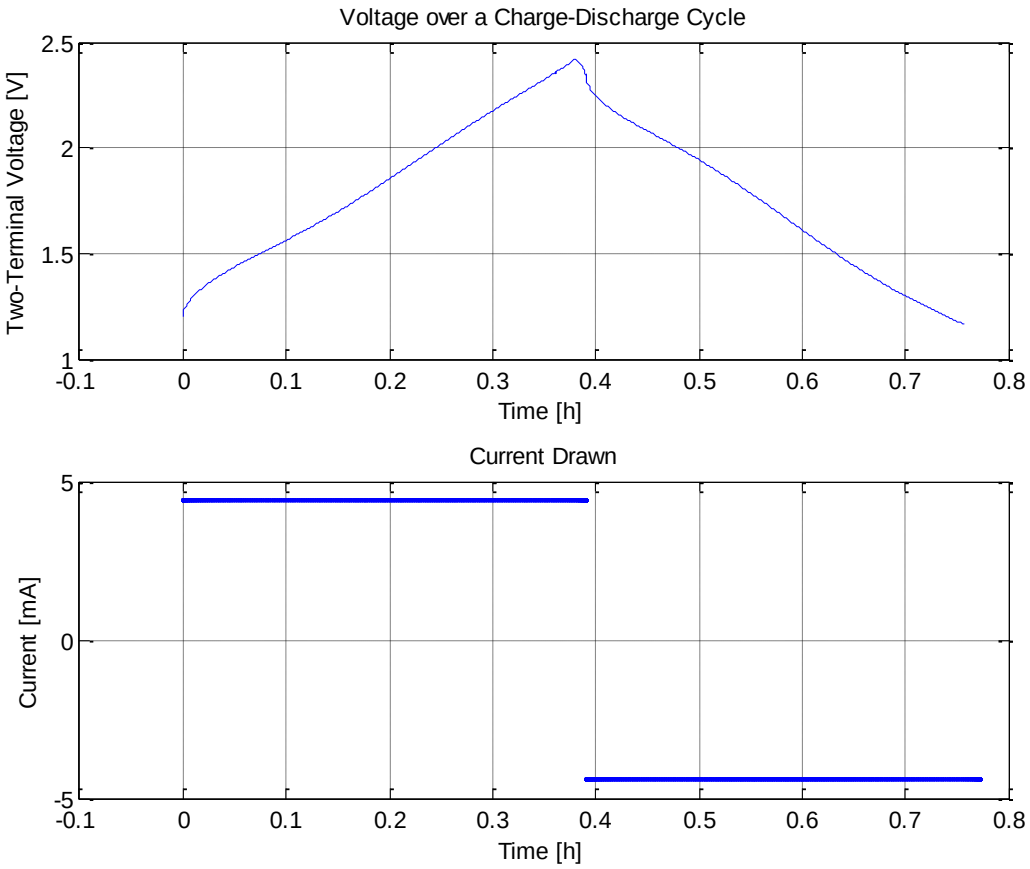

Fig. 3.4 Simulation of the full hybrid device undergoing a constant current charge-discharge test. The voltage of the polyaniline electrode, vs. lithium reference, is extracted from the cyclic voltammogram data for it, while the voltage of the lithium titanate electrode, vs. lithium reference, is obtained from Fig. 3.2. By subtracting the voltage of the lithium titanate electrode from that of the polyaniline electrode, the two-terminal voltage is obtained for various states of charge.

Since the voltage and current over this charge-discharge cycle are now simulated, the voltage is multiplied by the current to yield the instantaneous power over time and this is shown shown in Fig. 3.5.

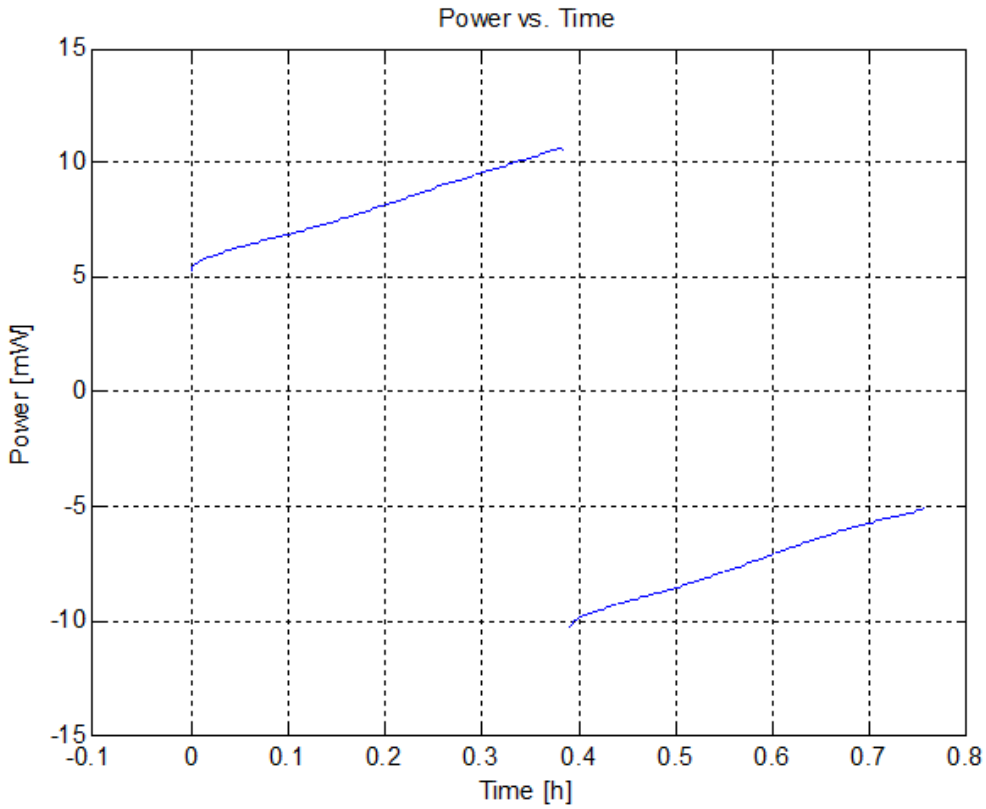

Fig. 3.5 Power into the cell over time in the charge-discharge test.

By integrating power over time for the charging cycle, the energy needed to charge the device is obtained. By integrating the power over time for the discharging cycle, the energy obtained from the device upon discharge is obtained.

The energy to charge the device is found to be 3.19 mWh. The energy obtained by discharging the capacitor was 2.75 mWh. Therefore, approximately 86.2% energy efficiency is obtained in the charge-discharge cycle.

The volume of the electrolyte is estimated by assuming that the charge transferred (approximately 1.68 mAh) must be accommodated by an electrolyte with a 1 M $LiPF_6$ concentration, as is commonly used for such applications [12]. Experimentally, the saturation concentration was found to be approximately 1.01 M, so the concentration of 1 M is close to saturation. The volume of electrolyte is determined as follows:

$$1.68\,mAh \times \frac{3.60\,C}{mAh} \times \frac{1\,elementary\ charge}{1.6\times10^{-19}\,C} \times \frac{1\,mol}{6.022\times10^{23}\,charges} \times \frac{1\,mL}{10^{-3}\,mol} = 62.9\,\mu L \ .$$

The mass of the full hybrid device must be estimated in order to calculate its energy density. In order to estimate this mass, the weight of the electrodes, the electrolyte, the separator and the stainless steel substrates must be added together.

The characteristics of the hybrid device simulated are summarized in Table 3.1 below. The energy density and cost characteristics of the device are summarized in Table 3.2 below. The details and assumptions used to produce these estimates are given in Appendix B.

Mass of Polyaniline	19.8 mg
Mass of Lithium Titanate	10.2 mg
Energy to charge device	3.19 mWh
Energy upon discharging device	2.75 mWh
Energy efficiency	86.2%

Table 3.1 Characteristics of Hybrid Device Simulated.

	Unit Cost	**Mass**	**Cost**
PANI	$6.78/kg	19.8 mg	0.0134 cents
Lithium Titanate	$10/kg	10.2 mg	0.0102 cents
Electrolyte: Acetonitrile	$1.30/L	44.4 mg	0.00735 cents
Electrolyte: $LiPF_6$	$75/kg	9.55 mg	0.0716 cents
Separator	-	1.36 mg	0.04 cents
Stainless Steel Foils	$3437/metric ton	31.6 mg	0.0109 cents
Packaging	-	3.79 mg	0.000546 cents
Total	-	**120.7 mg**	**0.154 cents**

Table 3.2 The cost and mass of the constituent materials of the above hybrid device are listed in this table. As stated above, this hybrid device is found to store 2.75 mWh of energy upon discharge.

Since the above device is found to store 2.75 mWh of energy upon discharge, the energy density is approximately 22.8 Wh/kg. This device has a cost of $560/kWh.

This energy density is more than two-thirds that of the lead acid battery which has an energy density of about 30 Wh/kg [23]. It is superior to using lithium titanate with carbon, which would only yield an energy density of 11 Wh/kg [24]. It is also superior to the hybrid device proposed by Du Pasquier *et al.* with polyfluorothiophene in conjunction with lithium titanate, which was reported to yield an energy density of only 6.1 to 7.4 Wh/kg [11]. However, it is still far less than the 130 Wh/kg energy density of a lithium-ion battery [23]. In terms of cost, the cost of $560/kWh is competitive with the lithium-ion battery, which has a cost figure of about $525/kWh (although this is expected to go down to less than $400/kWh in the next few years) [25]. However, it is higher than the cost figure for a lead-acid battery, which is around $150/kWh [26].

Nevertheless, the hybrid device should be useful for applications where device replacements are very difficult, as described in the introduction. In such applications, the lower energy density may be a worthwhile trade-off in favour of a longer lasting battery. Also, since capacitors are able to deliver greater power than batteries in short bursts, the hybrid device may be particularly useful in applications where vehicles are used in remote areas, since the capacitive nature of the device can help provide the surge currents needed to start motors. The low energy density compared to the lithium-ion battery is likely to be a significant obstacle preventing the widespread usage of the hybrid device in common applications. However, application in certain niche areas of industry is feasible and is worth exploring further.

4 Conclusions

The aim of this thesis has been to investigate the viability of combining a polyaniline electrode with a lithium titanate electrode in order to build an energy storage device with good energy density characteristics. The investigations in this thesis have shown that such a device is indeed a viable option.

Tests carried out on the polyaniline show that it is best fabricated from acidic aqueous solutions and that these samples can then be used in non-aqueous solutions to obtain good performance. The polyaniline electrode was shown to have a specific capacitance of approximately 220 F/g under such circumstances.

The test carried out on the lithium titanate electrode has enabled simulation of the full hybrid device with a polyaniline electrode and a lithium titanate electrode. Such a device is predicted to have an energy density of approximately 22.8 Wh/kg, which is slightly more than two-thirds that of lead acid battery technology, and may be useful in some remote applications. The cost of the device is estimated to be $560/kWh, which is reasonably competitive with the lithium ion battery but much higher than the lead-acid battery.

The device envisaged in this thesis is expected to have significantly longer lifetimes than batteries. However, in order to prove this, further testing is necessary under carefully controlled conditions. These tests will need to test the device for thousands of cycles over a very long time and were considered unfeasible for this thesis.

Some issues were encountered with the rapid degradation of the lithium titanate electrode, and these issues need to be resolved. The laboratory is currently working on this issue.

References

[1] B.E. Conway. (2003, March). *Electrochemical Capacitors: Their Nature, Function, and Applications* [Online]. Available: http://electrochem.cwru.edu/encycl/art-c03-elchem-cap.htm

[2] J. D.W. Madden, "Conducting Polymer Actuators," Ph.D. dissertation, Dept. Mech. Eng., Massachusetts Institute of Technology, Cambridge, MA, 2000.

[3] K.R. Prasad and N. Munichandraiah, "Fabrication and evaluation of 450F electrochemical redox supercapacitors using inexpensive and high-performance, polyaniline coated, stainless-steel electrodes," *J. Power Sources*, vol. 112, no. 2, pp. 443-451, Nov. 2002.

[4] A. Burke, "Ultracapacitors: why, how, and where is the technology," *J. Power Sources*, vol. 91, no. 1, pp. 37-50, Nov. 2000.

[5] Y.J. Kim *et al.*, "Correlation between the pore and solvated ion size on capacitance uptake of PVDC-based carbons," *Carbon*, vol. 42, no. 8-9, pp. 1491-1500, Mar. 2004.

[6] F. Fusalba *et al.*, "Electrochemical Characterization of Polyaniline in Nonaqueous Electrolyte and Its Evaluation as Electrode Material for Electrochemical Supercapacitors," *J. Electrochem. Soc.*, vol. 148, no. 1, pp. A1-A6, Jan. 2001.

[7] L. D. Johnson, private communication (quotation for aniline), Alfa Aesar, Ward Hill, MA, May 2006.

[8] L. D. Johnson, private communication (quotation for pyrrole), Alfa Aesar, Ward Hill, MA, May 2006.

[9] E. Frackowiak *et al.*, "Nanotubular materials for supercapacitors," *J. Power Sources*, vol. 97-98, pp. 822-825, Jul. 2001.

[10] M.C. Miras *et al.*, "Electroactive Polyaniline Film from Proton Free Nonaqueous Solution," *J. Electrochem. Soc.*, vol. 138, no. 1, Jan. 1991.

[11] A. Du Pasquier *et al*., "A Nonaqueous Asymmetric Hybrid $Li_4Ti_5O_{12}$/Poly(fluorophenylthiophene) Energy Storage Device," *J. Electrochem. Soc.*, vol. 149, no. 3, pp. A302-A306, Jan. 2002.

[12] K. Nakahara *et al.*, "Preparation of particulate $Li_4Ti_5O_{12}$ having excellent characteristics as an electrode active material for power storage cells," *J. Power Sources*, vol. 117, no. 1-2, pp. 131-136, May 2003.

[13] H. Yang and A.J. Bard, "The application of fast scan cyclic voltammetry. Mechanistic study of the initial stage of electropolymerization of aniline in aqueous solutions," *J. Electroanalytical Chemistry*, vol. 339, no.1-2, pp. 423-449, Nov. 1992.

[14] J.A. Raj *et al.*, "Electrochemical synthesis of nanosize polyaniline from aqueous surfactant solutions," *Materials Letters*, vol. 64, no. 8, pp. 895-897, Jan. 2010.

[15] T. Osaka *et al.*, "Electrochemical Polymerization of Electroactive Polyaniline in Nonaqueous Solution and Its Application in Rechargeable Lithium Batteries," *J. Electrochem. Soc.*, vol. 136, no. 2, Feb. 1989.

[16] N. Pekmez *et al.*, "The effect of monomer and acid concentrations on electrochemical polyaniline formation in acetonitrile," *J. Electroanalytical Chemistry*, vol. 353, no. 1-2, pp. 237-246, Jul. 1993.

[17] S.K. Mondal *et al.*, "Analysis of electrochemical impedance of polyaniline films prepared by galvanostatic, potentiostatic and potentiodynamic methods," *Synthetic Metals*, vol. 148, no. 3, pp. 275-286, Feb. 2005.

[18] K.S. Ryu *et al*., "Symmetric redox supercapacitor with conducting polyaniline electrodes," *J. Power Sources*, vol. 103, no. 2, pp. 305-309, Jan. 2002.

[19] J.H. Park and O.O. Park, "Hybrid electrochemical capacitors based on polyaniline and activated carbon electrodes," *J. Power Sources*, vol. 111, no. 1, pp. 185-190, Sep. 2002.

[20] G.E. Asturias and A.G. Macdiarmid, "The oxidation state of 'emeraldine' base," *Synthetic Metals*, vol. 29, no. 1, pp. E157-E162, Mar. 1989.

[21] A.G. Macdiarmid *et al.*, "Polyaniline: electrochemistry and application to rechargeable batteries," *Synthetic Metals*, vol. 18, no. 1-3, pp. 393-398, Feb. 1987.

[22] H. Tang, A. Kitani and Shiotani, M., "Effects of anions on electrochemical formation and overoxidation of polyaniline," *Electrochimica Acta*, vol. 41, no. 9, pp. 1561-1567, Jun. 1996.

[23] D. Linden and T.B. Reddy, *Handbook of Batteries*. New York: McGraw-Hill, 2002.

[24] I. Plitz *et al*., "The design of alternative nonaqueous high power chemistries," *Applied Physics A*, vol. 82, no. 4, pp. 615-626, Mar. 2006.

[25] R. Lache, D. Galves and P. Nolan. (2010, Mar. 7). *Vehicle Electrification* [Online]. Available: http://gm-volt.com/files/DB_EV_Growth.pdf

[26] D. Ton *et al.* (2008, May 6). *Solar Energy Grid Integration Systems – Energy Storage*. [Online]. Available: http://www1.eere.energy.gov/solar/pdfs/segis-es_concept_paper.pdf

[27] L. D. Johnson, private communication (quotation), Alfa Aesar, Ward Hill, MA, May 2006.

[28] B. Barnett *et al*., "PHEV Battery Cost Assessment," in *2010 DOE Vehicle Technologies and Hydrogen Programs Annual Merit Review and Peer Evaluation Meeting*, Washington, DC, Jun. 2010.

[29] (2011, May 6). *Lithium Hexafluorophosphate* [Online]. Available: http://www.sigmaaldrich.com/catalog/DisplayMSDSContent.do

[30] (2011, May 6). *Lithium Hexafluorophosphate* [Online]. Available: http://www.fluoridearc.com/product/Lithium-Hexafluorophosphate-battery-Grade.htm

[31] (2011, May 6). *Indicative Chemical Prices* [Online]. Available: http://www.icis.com/StaticPages/a-e.htm#A

[32] (2011, May 6). *Acetonitrile* [Online]. Available: http://www.sigmaaldrich.com/catalog/DisplayMSDSContent.do

[33] Mary. "Re: Bulk Quote Request for Lithium Hexafluorophosphate." E-mail (May 4, 2011).

[34] (2011, May 6). *Celgard Monolayer Polypropylene Separators* [Online]. Available: http://www.celgard.com/products/monolayer-pp.asp

[35] (2011, May 6). *Separators* [Online]. Available: http://www.gore.com/en_xx/products/electronic/battery/separators.html

[36] (2011, May 6). *Polypropylene Specifications* [Online]. Available: http://www.boedeker.com/polyp_p.htm

[37] F. Humiston. "celgard.com Contact Request from University of British Columbia." E-mail (May 10, 2011).

[38] (2011, May 6). *MEPS World Stainless Steel Prices* [Online]. Available: http://www.meps.co.uk/Stainless%20Prices.htm

[39] (2011, May 6). *304 Stainless Steel Material Property Data Sheet* [Online]. Available: http://www.suppliersonline.com/propertypages/304.asp

[40] (2011, May 6). *PlasticsUSA.com* [Online]. Available: http://www.plasticsusa.com/specgrav2.html

[41] (2011, May 6). *Market Study: Polypropylene* [Online]. Available: http://www.ceresana.com/en/market-studies/plastics/polypropylene

Appendices

Appendix A: Matlab Code for Full Device Simulation

This appendix gives the Matlab code used to simulate the full device based on the results obtained from polyaniline and lithium titanate testing. The simulation method used here is detailed in Chapter 3.

The code below loads the cyclic voltammogram data for the polyaniline and integrates current over time to find the charge transferred over time. Since the rate of change of voltage over time (dV/dt) is fixed, the time is related to the voltage of polyaniline in the cyclic voltammogram. Therefore, by relating charge transfer to time, the charge transfer is essentially related to the voltage of polyaniline. For any given state of charge for polyaniline, the data enables determination of the voltage of polyaniline (vs. lithium reference). The mass of polyaniline in the cyclic voltammogram is equal to the mass of polyaniline in the cell simulated.

As explained in Chapter 3, the code assumes that lithium titanate has a voltage of 1.58 V during charging and 1.54 V during discharging, versus lithium reference, since such an assumption is justified by the test results for the lithium titanate electrode.

By subtracting the voltage of the lithium titanate from the voltage of the polyaniline at various states of charge (vs. lithium reference), the two-terminal voltage of the hybrid device over time is determined, assuming that a fixed current is used to charge the device and then to discharge the device. This is plotted.

By multiplying the two-terminal voltage with the charging current followed by the discharging current, the instantaneous power over time is determined and plotted.

The power over time is then integrated for both the charging cycle and the discharging cycle in order to determine the energy needed to charge the device and the energy needed to discharge the device.

```
% Author: Rahul Krishna Prasad

clc; clear all; close all;

% Loading data for polyaniline
data = dlmread('5_8th_electrode_after_dep_PANI_SS_in_ACN_neg0_35V_to_0_95V_1mV_s.csv');

% Cyclic Voltammogram plot
figure(1)
plot(data(:,2),data(:,3))
title('Cyclic Voltammogram of PANI in Acetonitrile with 0.5M LiClO_4')
xlabel('Working Electrode Potential (V)')
ylabel('Current (A)')

% Integrating current to find Q as time progresses
data_Q = [];
for count=2:length(data)
    data_Q = [data_Q;trapz(data(1:count,1)-67.5,data(1:count,3))];
end
figure(2)
plot(data(2856:5682,1),data_Q(2856:5682)-data_Q(2856))

figure(3)
ref_elec_conv = 3.05; % 3.05V for conversion to Li+ ref. electrode
i = 4.4; % in mA
data_time = (data_Q(2856:4291)-data_Q(2856))./3.6./i;
subplot(2,1,1)
grid on
% plotting two-terminal voltage vs. time for charging
plot(data_time,data(2856:4291,2)+ref_elec_conv-1.58) % Li-Tit at 1.58V during charging
hold on;
xlabel('Time [h]')
ylabel('Two-Terminal Voltage [V]')
title('Voltage over a Charge-Discharge Cycle')
subplot(2,1,2)
grid on;

% plotting current vs. time for charging
plot(data_time,i,'b')
xlabel('Time [h]')
ylabel('Current [mA]')
title('Current Drawn')
hold on;

% plotting power vs. time for charging
figure(4)
plot(data_time,(data(2856:4291,2)+ref_elec_conv-1.58).*i)
trapz(data_time,(data(2856:4291,2)+ref_elec_conv-1.58).*i) % output energy stored on charging
hold on;

% plotting two-terminal voltage vs. time for discharging
```

```
figure(3)
data_time = 0.3914+0.3914-(data_Q(4291:5682)-data_Q(2856))./3.6./i;
subplot(2,1,1)
plot(data_time(1:5580-4291+1),data(4291:5580,2)+ref_elec_conv-1.54)

% plotting current vs. time for discharging
subplot(2,1,2)
plot(data_time,-i,'b')

% plotting power vs. time for discharging
figure(4)
hold on;
plot(data_time(1:5580-4291+1),(data(4291:5580,2)+ref_elec_conv-1.54).*-i)
trapz(data_time(1:5580-4291+1),(data(4291:5580,2)+ref_elec_conv-1.54).*-i) % output energy stored
on discharging
title('Power vs. Time')
xlabel('Time [h]')
ylabel('Power [mW]')
```

Appendix B: Details of Cost and Energy Density Calculations

This appendix shows the details of the cost and energy density calculations for the hybrid device.

The cost of polyaniline is estimated as being $6.78 per kilogram. This is based on a quote obtained from Alfa Aesar, Ward Hill, MA [7] that offers aniline at $6.78 per kilogram for a bulk order of 1070 kg. The process of synthesizing aniline into polyaniline will add to the cost, but this cost is likely to be minimal compared to the overall cost of the device.

The cost of lithium titanate was assumed to be $10/kg. This is based on a presentation at the 2010 U.S. D.O.E. Annual Merit Review for vehicle technologies. The figure is based on consultation with suppliers [28].

For 62.9 μL of electrolyte, with 1 M $LiPF_6$ concentration, 9.55 mg of $LiPF_6$ is needed since the molecular weight of $LiPF_6$ is 151.91 g/mol [29]. $LiPF_6$ has a density of 1.50 g/cm^3 [30], so 9.55 mg occupies 6.37 μL of space. Therefore, 56.5 μL of acetonitrile and 9.55 mg of $LiPF_6$ will form 62.9 μL of 1 M $LiPF_6$ solution.

The cost of the acetonitrile for the electrolyte was estimated as being $1.30 per litre. This is based on the published commercial price of $0.75 per pound on ICIS Chemical Business [31] and the density of acetonitrile, 0.786 g/mL, which was obtained from the MSDS for acetonitrile from Sigma-Aldrich, St. Louis, MO [32]. 56.5 μL of acetonitrile has a mass of 44.4 mg.

The cost of the $LiPF_6$ was estimated as $75 per kilogram based on a quote for bulk orders of 10 metric tons from Honest joy Holdings Limited/Shenzhen Feiyang Industry Co. Ltd., Shenzhen, China [33].

The separator is assumed to be made of polypropylene, as this material is used by Celgard LLC, Charlotte, NC and the thickness is assumed to be 25 μm [34]. The porosity is assumed to be 70%, which is typical for high porosity separators [35], so only 30% of the separator volume is made of polypropylene and the rest is empty space. The density of polypropylene is typically 0.905 g/cm^3 [36], so for a 2 cm x 1 cm separator, the mass is 1.36 mg. The cost is expected to be about $2.00 per square metre based on a quote from Celgard [37], so the cost of the separator for the cell is expected to be 0.04 cents.

Since this cell is very thin, a stainless steel foil of 10 μm thickness is used. The price of stainless steel (type 304) is $3437/metric ton [38] and its density is 7.9 g/cm^3 [39]. Two stainless steel foils are needed for the two electrodes, each of area 2 cm x 1 cm.

The above cell is very small. If it were to be commercialized, a very large number of such cells could be packed into a box. In order to obtain a very rough estimate of the packaging costs, it was assumed that a 20 cm x 20 cm x 20 cm box would be used for packaging. Since the cell described in this thesis uses stainless steel plates of 2 cm x 1 cm, one surface of this box would accommodate the equivalent of 200 cells. The polyaniline layer is approximately 100 μm thick and the electrolyte (without separator) would take up about 315 μm of thickness. With this information, it is estimated that each row of cells, after including the spacing between rows, would take up about 700 μm. Therefore, 285 rows of cells can be assembled, with each row being the equivalent of 200 of the cells described in this thesis. Therefore, this box would the equivalent of 57,000 of such cells. If the box is made of polypropylene and is 1 mm thick, then the volume of the packaging would be 240 cm^3. The density of polypropylene is 0.902 g/cm^3 [40]. Therefore, the packaging would have a mass of 0.216 kg. Estimating the cost to be $1.44/kg , the cost of the packaging would be $0.311 in this case. On average, for the equivalent of a single cell in this thesis, this corresponds to a mass of 3.79 mg and a cost of 0.000546 cents [41].